ACTA ABP BIOCHIMICA POLONICA

Vol. 70, No 3/2023
703–711
https://doi.org/10.18388/abp.2020_6511

Regular paper

Circ-PGPEP1 augments renal cell carcinoma proliferation, Warburg effect, and distant metastasis

PeiRui Wang[1#], Jin Chen[2#], Xin Ye[3], RuYi Wang[4], Lin Chen[4] and HanChao Zhang[4]✉

[1]Department of Urology, Affiliated Hospital of Zunyi Medical University, Zunyi City, Guizhou Province, 563000, China; [2]Department of Pediatric Surgery, Affiliated Hospital of Zunyi Medical University, Zunyi City, Guizhou Province, 563000, China; [3]Department of Urology, Institute of Urology, West China Hospital of Sichuan University, Chengdu City, Sichuan Province, 610000, China; [4]Department of Urology, Affiliated Hospital and Clinical Medical College of Chengdu University, Chengdu City, Sichuan Province, 610081, China

Circular RNAs (circRNAs) contribute to the malignant phenotype and progression of several types of human cancers, including renal cell carcinoma (RCC). This study probed the molecular mechanism of circPGPEP1 regulating RCC proliferation, Warburg effect, and distant metastasis by targeting the miR-378a-3p/JPT1 axis. Here identified higher circPGPEP1 expression in RCC tissues and cells by RT-qPCR, and high levels of circPGPEP1 were positively correlated with high histological grade and distant metastasis in RCC patients. Furthermore, patients with high levels of circPGPEP1 had a worse survival prognosis. Functional assays presented that knockdown of circPGPEP1 inhibited RCC proliferation, invasion, migration, EMT, and Warburg effect. Dual-luciferase reporter assay, RNA immunoprecipitation, nucleoplasmic RNA isolation, and functional rescue experiments confirmed that circPGPEP1 induced JPT1 expression by sponging miR-378a-3p, thereby promoting RCC malignant phenotype. Xenograft assays and metastasis models further demonstrated that down-regulation of circPGPEP1 effectively inhibited tumor growth and distant metastasis of RCC. Taken together, circPGPEP1, a prognostic circRNA in RCC, acts through the miR-378a-3p/JPT1 axis to regulate RCC progression.

Keywords: circSEC61A1, miR-378a-3p, JPT1, renal cell carcinoma, Warburg effect, distant metastasis

Received: 07 October, 2022; revised: 13 May, 2023; accepted: 24 May, 2023; available on-line: 18 September, 2023

✉e-mail: zhcandjay@163.com
#PeiRui Wang and Jin Chen contributed equally to this work.
Acknowledgements of Financial Support: Science Foundation of Affiliated Hospital and Clinical Medical College of Chengdu University (No. Y202207).
Abbreviations: circRNAs, Circular RNAs; miRNAs, microRNAs; RCC, Renal cell carcinoma

INTRODUCTION

Renal cell carcinoma (RCC) is the second leading cause of death in patients with urinary system tumors, accounting for about 3% of all adult malignant tumors (Scelo & Larose, 2018). Although partial and radical nephrectomy is the most effective treatment for early or localized RCC, approximately one-third of RCC patients are primarily diagnosed with advanced disease, and despite aggressive treatment, RCC at this stage has a low overall survival rate (Li *et al.,* 2020). In addition, recurrence and metastasis occur in approximately 30% of RCC patients (Choueiri & Motzer, 2017; Lara & Evans, 2019). RCC proliferation is a complex network involving multiple carcinogens and diverse genetic backgrounds, resulting in alterations in tumor suppressors or oncogenes (Moch *et al.,* 2014). There is a need to identify molecular mechanisms of RCC progression.

Circular RNAs (circRNAs) can be formed through back splicing events, in which upstream splice acceptor sites join with downstream splice donor sites, resulting in exon circularization (Yu *et al.,* 2020; Zhang *et al.,* 2014). Due to the stability and abundance of circRNAs, an increasing number of circRNAs have been identified to be aberrantly expressed in RCC (Zhou *et al.,* 2022). Mechanistically, these circRNAs act as sponges for microRNAs (miRNAs), thereby protecting downstream mRNAs from miRNAs-mediated degradation (Han *et al.,* 2018). For example, circ_0005875 knockdown suppresses RCC progression by regulating the miR-502-5p/ETS1 axis (Luo *et al.,* 2022). circNUP98, a potential biomarker, acts as an oncogene in RCC through the miR-567/PRDX3 axis (Yu *et al.,* 2020). circ_PGPEP1 is a sponge for miR-1297 and is involved in gastric carcinogenesis (Wang *et al.,* 2021). However, the role and mechanism of circPGPEP1 in RCC development remain to be explored.

Most malignancies are characterized by the Warburg effect (aerobic glycolysis), a unique mode of cellular metabolism in cancer cells that exhibits increased rates of glucose uptake and lactic acid fermentation in an aerobic environment (Cao *et al.,* 2020). Warburg effect has been intensively studied in the cellular progression of cancer cells over the past decade (Liberti & Locasale, 2016). circRNAs have been identified that can modulate the Warburg effect in human cancers (Li *et al.,* 2021), such as circRNA-FOXP1 (Fang *et al.,* 2021) and circ_0091579 (Chen *et al.,* 2021).

This study focused on the biological role of circPGPEP1 in RCC progression, and the Warburg effect, in combination with the regulatory network of circPGPEP1/miR-378a-3p/JPT1 involved in RCC. Taken together, these findings may provide new insights into the treatment of RCC.

MATERIALS AND METHODS

Clinical samples

Specimens were RCC tissue and adjacent normal renal tissue (>5 cm from cancer tissue) collected by radical or partial nephrectomy from 48 cases of RCC patients (no radiation or chemotherapy or other tumors) between 2013 and 2015 at Affiliated Hospital and Clinical Medical College of Chengdu University. Histological features of the specimens were confirmed by 2 pathologists. Dis-

tant metastases of tumor cells were evaluated by examining the lungs, liver, bone, intestine, and pancreas of patients with RCC. Samples were rapidly frozen at -80°C after enucleation for subsequent studies. This work was approved by the Ethics Committee of Affiliated Hospital and Clinical Medical College of Chengdu University and all patients gave written informed consent.

RT-qPCR

Total RNA acquisition was done with TRIzol® Reagent (Invitrogen, Thermo Fisher Scientific). RNA reverse transcription was performed at 37°C for 60 min using M-MLV buffers, dNTP and random primers, and Moloney Mouse leukemia virus RT kits (all from Promega, USA). Next, on a Bio-Rad CFX96 system (BioRad), PCR was done with SYBR Green Real-time PCR Master Mix (Solarbio, Beijing, China). Relative gene expression was determined using the $2^{-\Delta\Delta ct}$ method. The primer sequences are listed in Table 1. GAPDH and U6 were used as endogenous controls for genes.

Table 1. Primers in PCR

	Primer sequence (5′-3′)
GAPDH	Forward: 5′-GGAGCGAGATCCCTCCAAAAT-3′
	Reverse: 5′-GGCTGTTGTCATACTTCTCATGG-3′
U6	Forward: 5′-CTCGCTTCGGCAGCACA-3′
	Reverse: 5′-AACGCTTCACGAATTTGCGT-3′
CircPEPGP1	Forward: 5′-GTCTCGAACTCCTGACCTCA -3′
	Reverse: 5′-CACGGTGTGTTCCCCAAAAG-3′
miR-378a-3p	Forward: 5′-CGCGACTGGACTTGGAGTC-3′
	Reverse: 5′-AGTGCAGGGTCCGAGGTATT-3′
JPT1	Forward: 5′-AAGAACAGGTTTCTCTCTGTCCT-3′
	Reverse: 5′-AGCTTTCCCTCCAATCTACTACT-3′

Cell culture

Human renal tubular epithelial cell line (HK-2) and human RCC cell lines (786-O, ACHN, Caki1, Caki2, and 769-P) were obtained from ATCC and maintained in RPMI 1640 medium containing 10% FBS (Gibco), penicillin (100 U/ml) and streptomycin (100 μg/ml).

RNase R and Actinomycin D treatment

Extracted RNA (2 μg) from ACHN cells was treated with 3 U/μg RNase R (Epicenter Technologies). For the RNA stability assay, RNA extracted from ACHN cells was incubated with actinomycin D (Sigma-Aldrich) at 5 μg/ml for the indicated times. circPGPEP1 RNA expression levels were detected by RT-qPCR.

Cell transfection

To overexpress circPGPEP1 and JPT1, the overexpression plasmids of circPGPEP1 and JPT1 were constructed using the pcDNA 3.1 vector (Green Seed Biotech). siRNAs targeting circPGPEP1 and JPT1 were synthesized by Genepharm, while mimic/inhibitor (oligonucleotides) of miRNA and negative control were by RiboBio. The transfection reagent was Lipofectamine 2000 (Invitrogen).

Colony formation assay

Cells were maintained in DMEM containing 10% FBS for 2 weeks and those fixed in methanol were dyed with 1% crystal violet and counted under a microscope (Olympus).

Proliferation assay

A certain amount of 5-ethynyl-2'-deoxyuridine (EdU) solution (RiboBio) was added to each well containing 1×10^4 cells and incubated for 2 h. After being fixed with 4% paraformaldehyde, cells were reacted with glycine, 0.5% Triton X-100, and Apollo reaction solution until Hoechst 33342 staining and imaging under a fluorescence microscope.

Glucose uptake and lactate production

Cellular glucose uptake was quantified by Glucose Uptake Colorimetric Assay Kit (BioVision) (Qin *et al.,* 2021), while lactate concentration was by Lactate Assay Kit (K627, BioVision).

Extracellular acidification rate (ECAR)

ECAR (mpH/min) was determined by Seahorse Extracellular Flux Analyzer XF96 (Seahorse Bioscience) to reflect glycolytic activity in cells. 2×10^4 cells were grown overnight in 96-well plates and treated accordingly. Data were analyzed using Seahorse XF-96 Wave software.

Transwell

Cell migration and invasion were detected by transwell chambers with or without Matrigel (Corning Life Sciences, USA) (Zhu *et al.,* 2021). First, cells were added to 100 ml serum-free medium and seeded into the upper chamber, then 500 ml of DMEM with 10% serum were seeded into the lower chamber. Cells attached to the lower surface were then fixed with 4% paraformaldehyde after 24 h of incubation. After crystal violet staining, the samples were observed under a microscope and analyzed statistically.

Western blot

RIPA Lysis Buffer was utilized for the lysis of cells or tissues. Total protein was extracted and analyzed by the bicinchoninic acid assay (BCA) method to determine the protein quantity. The samples separated by 10% SDS-polyacrylamide gel electrophoresis were loaded onto a polyvinylidene fluoride membrane which was then supplementary to primary antibodies and the secondary antibody. Followed by visualization using ECL reagents (Millipore), the bands were evaluated by Image-Pro Plus 6.0 software. JPT1 (ab126705, Abcam), E-cadherin (3195, Cell Signaling Technology), N-cadherin (ab18203, Abcam), Snail (ab53519, Abcam), Ki-67 (ab15580, Abcam), HK2 (ab209847, Abcam), PKM2 (4053, Cell Signaling Technology), GAPDH (ab8245, Abcam) were used in the assay.

Nucleoplasmic RNA isolation

A nucleoplasmic RNA purification kit (Norgen Biotek Corp) was adopted to locate circPGPEP1 in cells. Afterward, concentrations of nuclear and cytoplasmic circPGPEP1 RNA were determined by RT-qPCR.

Dual-luciferase reporter assay

The circPGPEP1 and JPT1 3' UTR wild-type sequences (circPGPEP1/JPT1-WT) and their corresponding mutant sequences (circPGPEP1/JPT1-MUT) containing the miR-378a-3p binding site were synthesized. These sequences were each subcloned into psiCHECK2 (Promega) for subsequent co-transfection in ACHN cells using Lipofectamine 2000. Relative luciferase activity was determined using a dual luciferase assay system (Promega).

RNA immunoprecipitation (RIP)

RIP assays were implemented using the EZ Magna RIP kit (Millipore). Cell lysates were mixed with anti-Ago2 or anti-IgG (Millipore) before protein A/G (Thermo Fisher Scientific)-conjugated magnetic beads were added. Before the RT-qPCR assay, RNA purification was done with proteinase K.

Nude mouse xenograft experiments

The animal experiments were carried out after obtaining the approval of the Animal Ethics Committee of the Affiliated Hospital and Clinical Medical College of Chengdu University. ACHN cells (3×10^6 cells) stably transfected with si-NC or si-circPGPEP1 were inoculated subcutaneously into the right upper back of BALB/c mice (female, 6-week-old; n=5/treatment). The width and length of the tumor were measured at an interval of 1 week to calculate tumor volume as (length×width^2)/2. Tumor weight was assessed when the tumor was excised after 5 weeks. Gene expression was analyzed by IHC (Wang, Deng, *et al.,* 2020) or Western blot.

ACHN cells (2.5×10^6) stably knocked down circPGPEP1 were injected into the tail vein of nude mice. Livers and lungs were excised 7 weeks later to carry out HE staining to assess the number of metastatic nodules (Liu *et al.,* 2020).

Data analysis

Statistical analysis was performed using GraphPad Prism 9.0. Data are presented as mean ± standard deviation (S.D.). Chi-square testing assessed the association of circPGPEP1 with clinicopathological features, while the Kaplan-Meier method evaluated that of circPGPEP1 with RCC patients' survival. Statistical analysis between two groups was performed by Student's *t*-test, and that of multiple groups was by one-way analysis of variance (ANOVA). All experiments were performed with at least three biological replicates. $P<0.05$ was considered statistically significant.

RESULTS

High circPGPEP1 level is associated with poor prognosis in RCC patients

To investigate whether circPGPEP1 has a biological function in RCC, circPGPEP1 expression in RCC tissues was evaluated by RT-qPCR. As measured, circPGPEP1 expression was up-regulated in patients' tumor tissues compared with normal tissues (Fig. 1A). circPGPEP1 in RCC cell lines was subsequently evaluated. The results showed that circPGPEP1 expression in the five RCC cell lines was higher than in HK-2 cells, and circPGPEP1 expression was the highest in ACHN cells (Fig. 1B).

In accordant with the bioinformatics website circbase, circPGPEP1 is located on chromosome 19p13.11 with a length of 557 bp (Fig. 1C). RNase R and actinomycin D treatment identified the ring structure of circPGPEP1. As reflected in Fig. 1D, E. RNase R and actinomycin D treatments decreased the expression and half-life of the linear RNA GAPDH mRNA, respectively, but not circPGPEP1.

Subsequently, RCC patients were divided into a high circPGPEP1 expression group and a low circPGPEP1 expression group according to the median expression of circPGPEP1 in RCC patients. The association of circPGPEP1 with clinicopathologic features in patients with RCC was evaluated. As listed in Table 2, high levels of circPGPEP1 were positively correlated with high histological grade and distant metastasis in RCC patients. The relationship between circPGPEP1 and survival outcomes in patients with RCC was evaluated by Kaplan-Meier. Patients with high levels of circPGPEP1 had a worse survival prognosis (Fig. 1F). Briefly, aberrant ex-

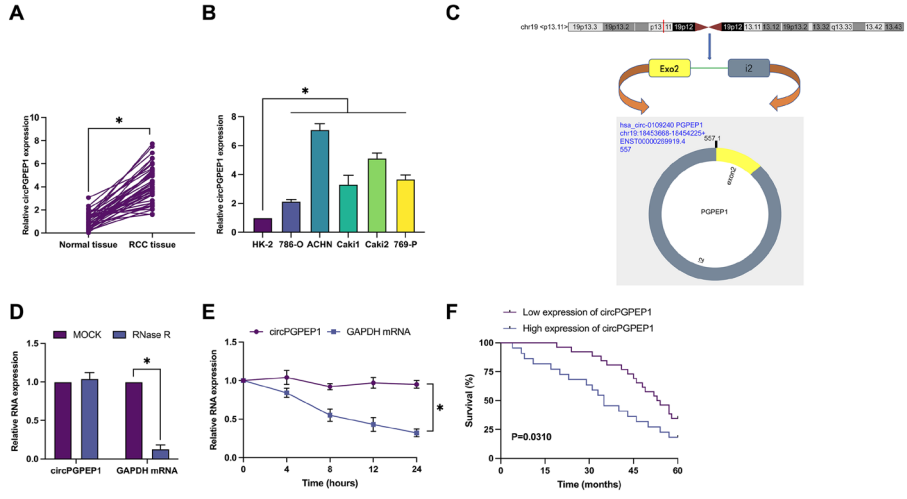

Figure 1. High circPGPEP1 level is associated with poor prognosis in RCC patients
(**A**) RT-qPCR detection of circPGPEP1 expression in RCC tissues and normal tissues; (**B**) RT-qPCR detection of circPGPEP1 expression in RCC cell lines and HK-2 cells; (**C**) circPGPEP1 gene information on circbase; (**D**) RNase R experiment tested circPGPEP1 ring structure; (**E**) Actinomycin D treatment analyzed the stability of circPGPEP1; (**F**) circPGPEP1 expression and survival prognosis of RCC patients; data representation = mean ± S.D. (N=3); $P<0.05$.

Table 2. Relationship between circPGPEP1 and clinicopathological features of RCC patients

Characteristic	Cases	circPGPEP1 expression		P
	n = 48	Low (n = 24)	High (n = 24)	
Age (year)				
≤ 60	14	5	9	0.2042
> 60	34	19	15	
Tumor size				
< 3 cm	19	7	12	0.14
≥ 3 cm	29	17	12	
FIGOa stage				
I-II	28	21	7	<0.0001*
II-IV	20	3	17	
Lymph node metastasis				
Positive	25	14	11	0.3861
Negative	23	10	13	
Distant metastasis				
Positive	10	2	8	0.0330*
Negative	38	22	16	

pression of circPGPEP1 is related to the malignant progression of RCC.

Knockdown of circPGPEP1 inhibits RCC cell proliferation, invasion, migration, EMT, and Warburg effect

Next, the biological function of circPGPEP1 in RCC cells was explored. CircPGPEP1-targeting siRNA was transfected into ACHN cells to knock down circPGPEP1 (Fig. 2A). The proliferation ability of cells was first evaluated by colony formation assay and EdU assay. The clonogenic ability of cells decreased and the ratio of EdU-positive cells decreased after the down-regulation of circPGPEP1 (Fig. 2B, C). The invasive and migratory abilities were subsequently assessed by Transwell, and it was found that knocking down circPGPEP1 reduced the number of cells invaded and migrated (Fig. 2D). Since EMT is a key process in the distant metastasis of cancer

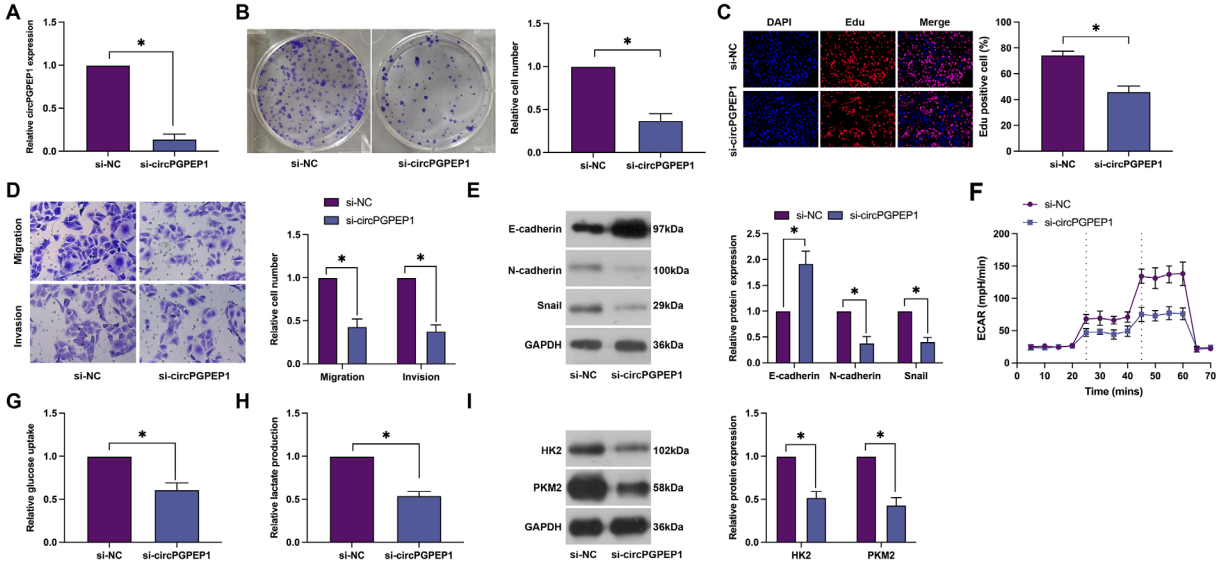

Figure 2. Silencing circPGPEP1 inhibits RCC cell proliferation, invasion, migration, EMT, and Warburg effect
CircPGPEP1-targeting siRNA was transfected into ACHN cells. (**A**) RT-qPCR analyzed the knockdown efficiency of si-circPGPEP1; (**B–C**) Colony formation assay and EdU assay tested analyzed proliferation ability; (**D**) Transwell assay tested invasion and migration ability; (**E**) Immunoblot assayed protein expression of EMT-related proteins (E-cadherin, N-cadherin, and Snail); (**F**) cellular ECAR; (**G**) glucose uptake; (**H**) lactate production capacity; (**I**) Immunoblot assayed protein expression of aerobic glycolysis-related proteins (HK2 and PKM2); data representation = mean ± S.D. (N=3); $P<0.05$.

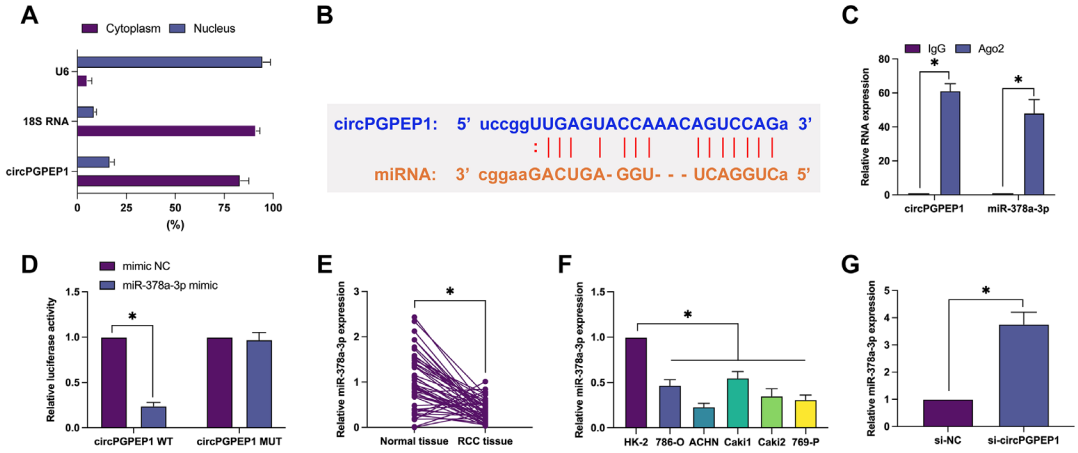

Figure 3. Competitive adsorption of miR-378a-3p by circPGPEP1
(**A**) Nucleoplasmic RNA isolation assay analyzed the subcellular localization of circPGPEP1 in ACHN cells; (**B**) Potential binding sites of circPGPEP1 and miR-378a-3p; (**C**) RIP experiment checked the binding relationship between circPGPEP1 and miR-378a-3p; (**D**) Dual luciferase reporter assay tested the targeting relationship between circPGPEP1 and miR-378a-3p; (**E**) RT-qPCR tested miR-378a-3p expression in RCC tissues and normal tissues; (**F**) RT-qPCR tested miR-378a-3p expression in RCC cell lines and HK-2 cells; (**G**) RT-qPCR tested miR-378a-3p expression in ACHN cells after knockdown of circPGPEP1; data representation = mean ± S.D. (N=3); $P<0.05$.

cells, EMT-related proteins were evaluated by immunoblot. It was presented that knockdown of circPGPEP1 suppressed N-cadherin and Snail and promoted E-cadherin expression (Fig. 2E). Warburg effect is an important way for cancer cells to acquire capacity through aerobic glycolysis (Vaupel & Multhoff, 2021). Therefore, changes in the Warburg effect were observed in RCC cells after interfered with circPGPEP1. As reported in Fig. 2F–H, ECAR, glucose uptake, and lactate production were reduced after the knockdown of circPGPEP1 (Fig. 2F–H). The expression of proteins associated with aerobic glycolysis was then evaluated. Knockdown of circPGPEP1 inhibited the expression of HK2 and PKM2 proteins (Fig. 2I).

Competitive adsorption of miR-378a-3p by circPGPEP1

Our research focus was shifted to the downstream molecules of circPGPEP1. The subcellular localization of circPGPEP1 was first assessed, finding that circPG-

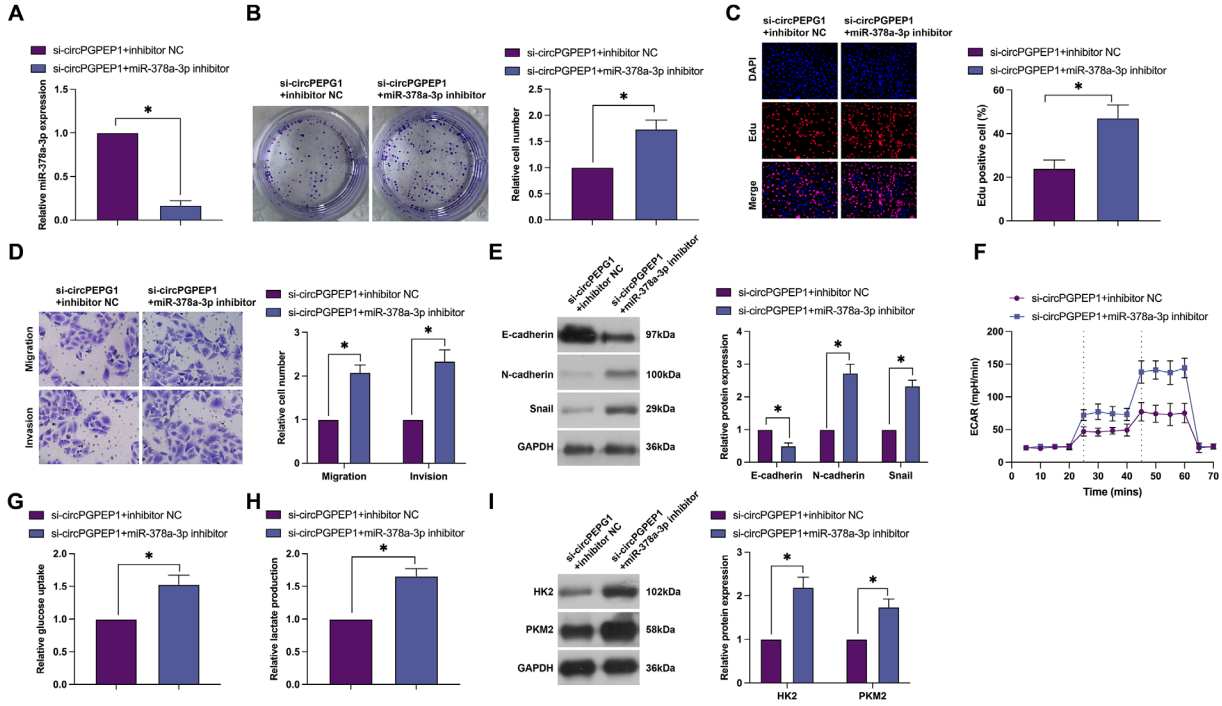

Figure 4. miR-378a-3p contributes to a reversal of effects of si-circPGPEP1 on RCC
si-circPGPEP1 and miR-378a-3p inhibitor were co-transfected into ACHN cells for functional rescue experiments. (**A**) RT-qPCR tested miR-378a-3p expression; (**B–C**) Colony formation assay and EdU assay tested analyzed proliferation ability; (**D**) Transwell assay tested invasion and migration ability; (**E**) Immunoblot assayed protein expression of EMT-related proteins (E-cadherin, N-cadherin, and Snail); (**F**) cellular ECAR; (**G**) glucose uptake; (**H**) lactate production capacity; I: Immunoblot assayed protein expression of aerobic glycolysis-related proteins (HK2 and PKM2); data representation = mean ± S.D. (N=3); $P<0.05$.

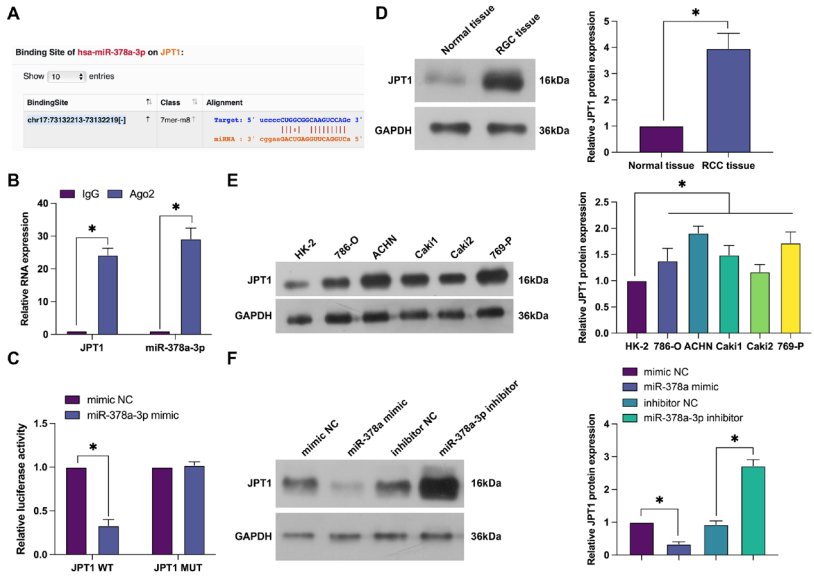

Figure 5. miR-378a-3p targets JPT1 expression
(**A**) Potential binding sites of JPT1 and miR-378a-3p; (**B**) RIP assay analyzed the binding relationship between JPT1 and miR-378a-3p; (**C**) Dual luciferase reporter assay analyzed the targeting relationship between JPT1 and miR-378a-3p; (**D**) Immunoblot assayed JPT1 protein expression in RCC tissues and normal tissues; (**E**) Immunoblot assayed JPT1 protein expression in RCC cell lines and HK-2 cells; (**F**) Immunoblot assayed JPT1 protein expression in ACHN cells after lowering or overexpressing miR-378a-3p; data representation = mean ± S.D. (N=3); $P<0.05$.

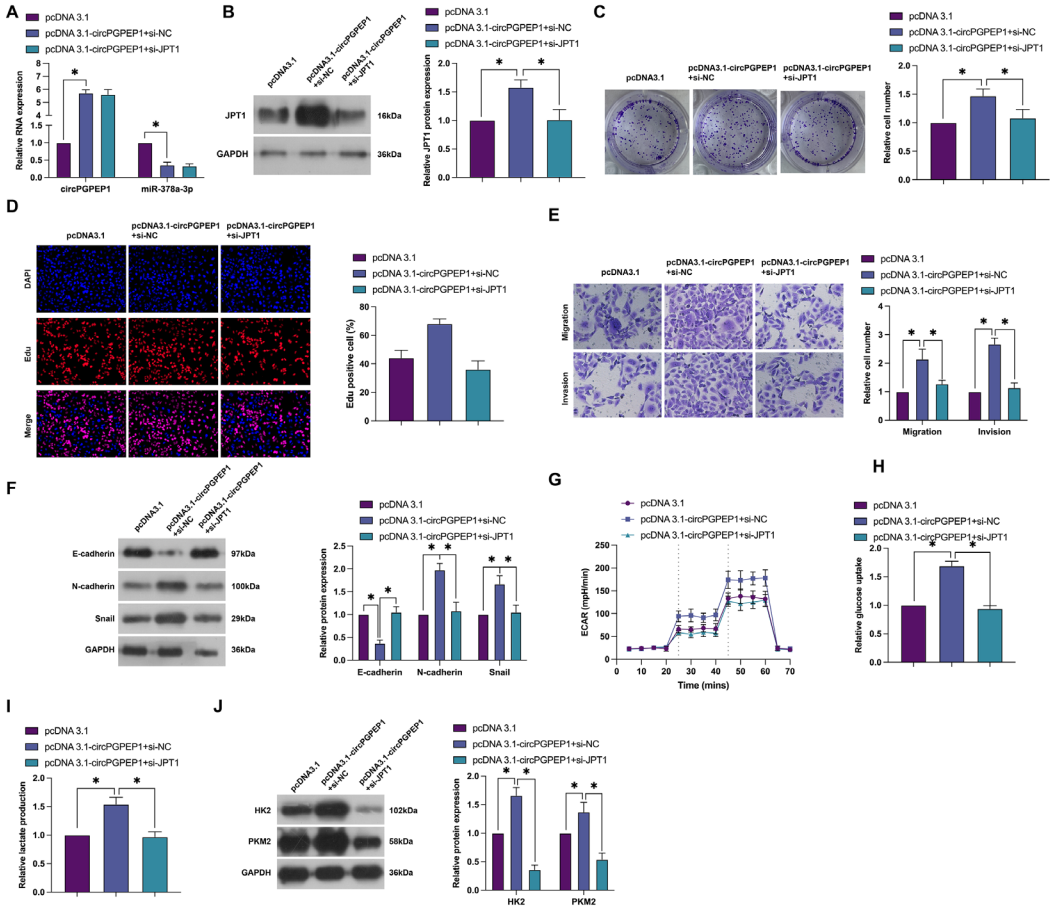

Figure 6. circPGPEP1 affects RCC progression by miR-378a-3p/JPT1 axis
pcDNA 3.1-circPGPEP1 and si-JPT1 were co-transfected into ACHN cells for functional rescue experiments. (**A**) RT-qPCR tested circPGPEP1 and miR-378a-3p expression; (**B**) Immunoblot assayed JPT1 protein expression; (**C–D**) Colony formation assay and EdU assay tested analyzed proliferation ability; (**E**) Transwell assay tested invasion and migration ability; (**F**) Immunoblot assayed protein expression of EMT-related proteins (E-cadherin, N-cadherin, and Snail); (**G**) cellular ECAR; (**H**) glucose uptake; (**I**) lactate production capacity; (**J**) Immunoblot assayed protein expression of aerobic glycolysis-related proteins (HK2 and PKM2); data representation = mean ± S.D. (N=3); $P<0.05$.

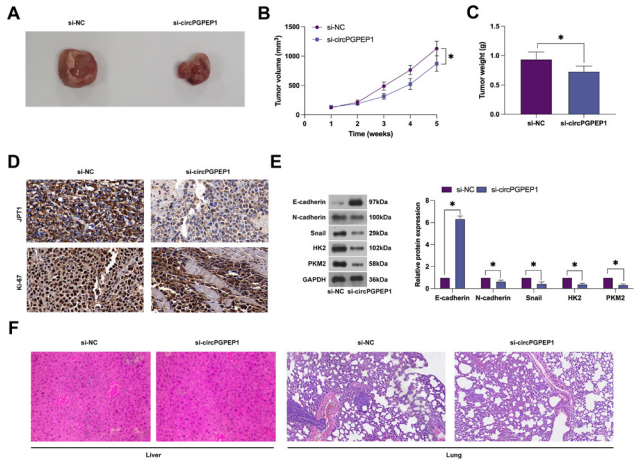

Figure 7. circPGPEP1 promotes RCC tumor growth and distant metastasis in vivo
ACHN cells with stable knockdown of circPGPEP1 were injected subcutaneously or intravenously into nude mice to evaluate tumor growth and distant metastasis. (**A**) representative image of tumor; (**B–C**) tumor volume and weight: (**D**) IHC staining evaluated tumor JPT1 and Ki-67 expression; (**E**) Immunoblot assayed E-cadherin, N-cadherin, Snail, HK2, and PKM2 proteins level in tumors; (**F**) HE staining assessed the ability of the tumor to metastasize to lung and liver; data representation = mean ± S.D. (n=5); $P<0.05$.

PEP1 was mainly localized in the cytoplasm of ACHN cells (Fig. 3A), which suggested that circPGPEP1 mediates gene expression mainly by targeting and adsorbing miRNAs. The bioinformatics website https://starbase.sysu.edu.cn predicted 10 miRNAs with potential binding sites for circPGPEP1, which were screened by RIP experiments to find that miR-378a-3p and circPGPEP1 were enriched in the Ago2 precipitation complex (Fig. 3B, C). Their targeting relationship was further examined by dual-luciferase, showing that when miR-378a-3p was overexpressed, the luciferase activity decreased in circPGPEP1 WT (Fig. 3D). Subsequently, the expression of miR-378a-3p in RCC was evaluated. Both RCC tissues and RCC cell lines expressed miR-378a-3p at a low level (Fig. 3E, F). Interestingly, miR-378a-3p expression was effectively restored in ACHN cells after knockdown of circPGPEP1 (Fig. 3G). These data suggest that circPGPEP1 binds to miR-378-3p in RCC and regulates miR-378a-3p expression.

miR-378a-3p contributes to a reversal of the effects of si-circPGPEP1 on RCC

miR-378a-3p inhibitor was simultaneously transfected in ACHN cells transfected with si-circPGPEP1 to determine whether circPGPEP1 affects RCC development by regulating miR-378a-3p. The promoting effect of si-circPGPEP1 on miR-378a-3p expression was restrained by miR-378a-3p inhibitor (Fig. 4A). Furthermore, functional experiments observed that the preventive effects of si-circPGPEP1 on ACHN cell proliferation, invasion and migration, EMT, and aerobic glycolysis were all blocked after co-transfection of miR-378a-3p inhibitor (Fig. 4B–I). These data suggest that circPGPEP1 affects the biological behavior of RCC by regulating the expression of miR-378a-3p.

miR-378a-3p targets JPT1 expression

Next, the downstream target genes of miR-378a-3p were explored. The bioinformatics website https://starbase.sysu.edu.cn found 10 mRNAs with potential binding sites for miR-378a-3p. Among them, JPT1 was found to be significantly enriched with miR-378a-3p in the Ago2 precipitation complex in ACHN cells (Fig. 5A, B). Dual luciferase reporter experiments showed that co-transfection of JPT1 WT with miR-378a-3p mimic mediated a decrease in the luciferase activity (Fig. 5C). Subsequently, the expression of JPT1 in RCC was explored by immunoblot. JPT1 protein expression was higher in RCC tissues and cells than in normal tissues or cells (Fig. 5D, E). In addition, decreased or increased expression of JPT1 was detected in ACHN cells overexpressing or knocking down miR-378a-3p, respectively (Fig. 5F). These data suggest that targeting miR-378a-3p regulates JPT1 expression.

circPGPEP1 affects RCC progression *via* miR-378a-3p/JPT1 axis

To test the conjecture that circPGPEP1 affects RCC progression by miR-378a-3p/JPT1 axis, si-JPT1 was introduced in ACHN cells overexpressing circPGPEP1. Overexpressing circPGPEP1 promoted circPGPEP1 and JPT1 levels and inhibited miR-378a-3p expression. si-JPT1 decreased JPT1, but did not affect circPGPEP1 and miR-378a-3p levels (Fig. 6A, B). Furthermore, circPGPEP1 overexpression increased cell colony-forming ability and EdU-positive cell rate but knocking down JPT1 prevents these changes (Fig. 6C, D). Transwell assay and immunoblot showed that circPGPEP1 overexpression increased the number of invasive and migratory cells and N-cadherin and Snail protein expression, but JPT1 knockdown reversed these phenomena (Fig. 6E, F). Furthermore, the stimulative effect of circPGPEP1 overexpression on aerobic glycolysis was impeded by knocking down JPT1 (Fig. 6G–J). These data suggest that circPGPEP1 promotes RCC proliferation, invasion, migration, EMT, and Warburg effect by regulating the miR-378a-3p/JPT1 axis.

circPGPEP1 promotes RCC tumor growth and distant metastasis *in vivo*

In vivo experiments were included to further support the above *in vitro* results. Tumor growth and distant metastasis were assessed by subcutaneous inoculation or tail vein injection of ACHN cells stably knocking down circPGPEP1 into nude mice. Depleting circPGPEP1 suppressed tumor volume and weight (Fig. 7A–C).

IHC staining showed that knockdown of circPGPEP1 inhibited JPT1 and Ki-67 positive cell ratio in tumors (Fig. 7D). Immunoblot found that depleting circPGPEP1 reduced N-cadherin, Snail, HK2, and PKM2 protein levels, and elevated E-cadherin protein levels (Fig. 7E). HE staining exhibited that silencing circPGPEP1 reduced the number of lung and liver metastatic nodules (Fig. 7F). These data suggest that down-regulating circPGPEP1 effectively inhibits tumor growth and distal metastasis of RCC.

DISCUSSION

RCC is a malignancy in the urinary system that has a poor prognosis despite improved treatments **(15)**. The plight of RCC treatment makes it necessary to further explore its mechanism and find effective RCC therapeutic targets. Recently, circRNAs have been intensively studied as a promising direction for gene-targeted therapy (Wang *et al.,* 2020). In line with this, the circPGPEP1-oriented mechanism in RCC was probed through miR-378a-3p/JPT1.

CircPGPEP1 was stably and highly expressed in human RCC tissues and cells, and high levels of circPGPEP1 were associated with poor clinicopathological features and prognosis in RCC patients. Recently, a large number of studies have proposed that circRNAs are involved in the malignant progression in RCC, such as circNUP98 (Yu *et al.,* 2020), Circ_0005875 (Luo *et al.,* 2022), Circ-EGLN3 (Zhang *et al.,* 2021), etc., which are highly expressed in RCC cells and are closely related to the growth and metastasis of RCC. Wang *et al.,* disclosed that circPGPEP1 silencing hampers pro-apoptosis, migration, and invasion of cancer cells, and reduces tumor growth *in vivo* (Wang *et al.,* 2021). In the present study, circPGPEP1 silencing led to a reduction of cell proliferation, invasion, and migration in RCC cells. Influences of circPGPEP1 on EMT-related proteins were studied since EMT is a key process in the distant metastasis of cancer cells (Piva *et al.,* 2016), which showed that circPGPEP1 silencing inhibited EMT progression. Tumor cells obtain energy through the Warburg effect to maintain tumor development (Liberti and Locasale 2016) and circRNAs enable themselves to mediate the Warburg effect in RCC (Li *et al.,* 2021). Here, our study confirmed that down-regulated circPGPEP1 inhibited the Warburg effect in RCC cells. Additionally, inhibiting circPGPEP1 could effectively inhibit the tumor growth and distant metastasis of RCC, further reflecting the tumor-promoting action of circPGPEP1 in RCC. Recently, it has been gradually discovered that circRNAs in exosomes act in intercellular communication, tumor immune response, tumor cell migration, and invasion (Liu *et al.,* 2021). Therefore, RCC cell exosomes can be a study target in subsequent studies.

CircRNAs have been widely demonstrated to act as ceRNAs to counteract the effects of miRNAs (Jorgensen and Ro 2022). Accumulated miRNAs have conferred regulatory influences on RCC metastasis, implicated in a variety of cellular processes, including proliferation, migration, invasion, EMT, and Warburg effect (Abozed *et al.,* 2017). It is known that miR-378a-3p expresses differentially in cancers, including hepatocellular carcinoma (Li *et al.,* 2022), prostate cancer (Cannistraci *et al.,* 2022), breast cancer (Niu *et al.,* 2021), etc. Notably, miR-378a-5p is considered a tumor suppressor in RCC and correlates with a good prognosis for patients (Pan *et al.,* 2019). The present study focused on miR-378a-3p and revealed that miR-378a-3p was down-regulated in RCC. miR-376a-3p could be targeted and regulated by circRNA and then involved in cancer progression (Mao *et al.,* 2020). More importantly, the present study confirmed that circPGPEP1 mainly mediates gene expression by absorbing miRNAs, and circPGPEP1 affects RCC development by regulating miR-378a-3p. In detail, the preventive influences of silencing circPGPEP1 on RCC cells were all hampered when miR-378a-3p was inhibited.

miRNAs are widely involved in cancer promotion and repression by regulating cancer-related genes (Abozed *et al.,* 2017). JPT1 is a ~16 kDa protein (Q9UK76, uniprot.org) that was originally identified as an abundant transcript in mouse hematopoietic and brain cells (Bateman *et al.,* 2020; Tang *et al.,* 1997). Notably, JPT1 is abnormally high expressed in cancers. For example, JPT1 expression is 3 times higher in ovarian cancer cells than in normal ovarian epithelial cells (Lu *et al.,* 2004). In glioma, lowering JPT1 reduces tumor growth (Laughlin *et al.,* 2009). In addition, JPT1 can interact with STMN1 to promote the growth and metastasis of thyroid anaplastic carcinoma (Pan *et al.,* 2021). Likewise, the present study noted that JPT1 was upregulated in RCC and JPT1 acted as an oncogene in RCC. Knockdown of JPT1 reversed the promotion effect of circPGPEP1 overexpression on proliferation, invasion, migration, EMT, and glycolysis of RCC cells. This suggests that circPGPEP1 plays a role in promoting cancer by up-regulating JPT1 expression.

Although the circPGPEP1/miR-378a-3p/JPT1 axis-related mechanism in RCC progression has been partially elucidated, further investigation is still required. For example, it is necessary to further determine circPGPEP1 pattern in the serum of RCC patients and to determine the potential of circEHD2 as a diagnostic biomarker for RCC. Furthermore, the downstream pathways of JPT1 in RCC cell progression need to be further elucidated.

CONCLUSION

Our findings suggest that circPGPEP1 is an "oncogene" in RCC. Highly circPGPEP1 promotes cell proliferation and metastasis through miR-378a-3p-mediated JPT1. Our findings not only explain the mechanism of circPGPEP1 in regulating RCC cell progression but also provide potential therapeutic targets for RCC.

Declarations

Acknowledgments. Not applicable.

Competing interests. The authors have no conflicts of interest to declare.

Data available. Data is available from the corresponding author on request.

REFERENCES

Abozed M, Alsulaiti G, Almannaei F, Raza A, El Beltagi A, Ayyad A (2017) Anterior clinoid mucocele causing optic neuropathy: A case report and review of literature. *eNeurologicalSci* **7**: 57–59. https://doi.org/10.1016/j.ensci.2017.05.005

Bateman NW, Teng PN, Hope E, Hood BL, Oliver J, Ao W, Zhou M, Wang G, Tommarello D, Wilson K, Litzy T, Conrads KA, Hamilton CA, Darcy KM, Casablanca Y, Maxwell GL, Bae-Jump V, Conrads TP (2020) Jupiter microtubule-associated homolog 1 (JPT1): A predictive and pharmacodynamic biomarker of metformin response in endometrial cancers. *Cancer Med* **9**: 1092–1103. https://doi.org/10.1002/cam4.2729

Cannistraci A, Hascoet P, Ali A, Mundra P, Clarke NW, Pavet V, Marais R (2022) MiR-378a inhibits glucose metabolism by suppressing GLUT1 in prostate cancer. *Oncogene* **41**: 1445–1455. https://doi.org/10.1038/s41388-022-02178-0

Cao L, Wang M, Dong Y, Xu B, Chen J, Ding Y, Qiu S, Li L, Karamfilova Zaharieva E, Zhou X, Xu Y (2020) Circular RNA circRNF20 promotes breast cancer tumorigenesis and Warburg effect through miR-487a/HIF-1α/HK2. *Cell Death Dis* **11**: 145. https://doi.org/10.1038/s41419-020-2336-0

Chen Y, Song S, Zhang L, Zhang Y (2021) Circular RNA hsa_circ_0091579 facilitates the Warburg effect and malignancy of hepatocellular carcinoma cells *via* the miR-624/H3F3B axis. *Clin Transl Oncol* **23**: 2280–2292. https://doi.org/10.1007/s12094-021-02627-4

Choueiri TK, Motzer RJ (2017) Systemic therapy for metastatic renal-cell carcinoma. *N Engl J Med* **376**: 354–366. https://doi.org/10.1056/NEJMra1601333

Fang L, Ye T, An Y (2021) Circular RNA FOXP1 induced by ZNF263 upregulates U2AF2 expression to accelerate renal cell carcinoma tumorigenesis and Warburg effect through sponging miR-423-5p. *J Immunol Res* **2021**: 8050993. https://doi.org/10.1155/2021/8050993

Han B, Chao J, Yao H (2018) Circular RNA and its mechanisms in disease: From the bench to the clinic. *Pharmacol Ther* **187**: 31–44. https://doi.org/10.1016/j.pharmthera.2018.01.010

Jorgensen BG, Ro S (2022) MicroRNAs and 'Sponging' competitive endogenous RNAs dysregulated in colorectal cancer: potential as noninvasive biomarkers and therapeutic targets. *Int J Mol Sci* **23**. https://doi.org/10.3390/ijms23042166

Lara PN, Jr, Evans CP (2019) Cytoreductive nephrectomy in metastatic renal cell cancer: not all that it's cut out to be. *JAMA Oncol* **5**: 171–172. https://doi.org/10.1001/jamaoncol.2018.5503

Laughlin KM, Luo D, Liu C, Shaw G, Warrington KH, Jr, Qiu J, Yachnis AT, Harrison JK (2009) Hematopoietic- and neurologic-expressed sequence 1 expression in the murine GL261 and high-grade human gliomas. *Pathol Oncol Res* **15**: 437–444. https://doi.org/10.1007/s12253-008-9147-4

Li J, Huang C, Zou Y, Yu J, Gui Y (2020) Circular RNA MYLK promotes tumour growth and metastasis *via* modulating miR-513a-5p/VEGFC signalling in renal cell carcinoma. *J Cell Mol Med* **24**: 6609–6621. https://doi.org/10.1111/jcmm.15308

Li T, Xian HC, Dai L, Tang YL, Liang XH (2021) Tip of the Iceberg: roles of CircRNAs in cancer glycolysis. *Onco Targets Ther* **14**: 2379–2395. https://doi.org/10.2147/ott.S297140

Li Y, Zhou T, Cheng X, Li D, Zhao M, Zheng WV (2022) microRNA-378a-3p regulates the progression of hepatocellular carcinoma by regulating PD-L1 and STAT3. *Bioengineered* **13**: 4730–4743. https://doi.org/10.1080/21655979.2022.2031408

Liberti MV, Locasale JW (2016) The Warburg effect: how does it benefit cancer cells? *Trends Biochem Sci* **41**: 211–218. https://doi.org/10.1016/j.tibs.2015.12.001

Liu J, Ren L, Li S, Li W, Zheng X, Yang Y, Fu W, Yi J, Wang J, Du G (2021) The biology, function, and applications of exosomes in cancer. *Acta Pharm Sin B* **11**: 2783–2797. https://doi.org/10.1016/j.apsb.2021.01.001

Liu S, Wu M, Peng M (2020) Circ_0000260 Regulates the development and deterioration of gastric adenocarcinoma with cisplatin resistance by upregulating MMP11 *via* targeting MiR-129-5p. *Cancer Manag Res* **12**: 10505–10519. https://doi.org/10.2147/cmar.S272324

Lu KH, Patterson AP, Wang L, Marquez RT, Atkinson EN, Baggerly KA, Ramoth LR, Rosen DG, Liu J, Hellstrom I, Smith D, Hartmann L, Fishman D, Berchuck A, Schmandt R, Whitaker R, Gershenson DM, Mills GB, Bast RC, Jr (2004) Selection of potential markers for epithelial ovarian cancer with gene expression arrays and recursive descent partition analysis. *Clin Cancer Res* **10**: 3291–3300. https://doi.org/10.1158/1078-0432.Ccr-03-0409

Luo S, Deng F, Yao N, Zheng F (2022) Circ_0005875 sponges miR-502-5p to promote renal cell carcinoma progression through upregulating E26 transformation specific-1. *Anticancer Drugs* **33**: e286–e298. https://doi.org/10.1097/cad.0000000000001205

Mao Y, Li W, Hua B, Gu X, Pan W, Chen Q, Xu B, Lu C, Wang Z (2020) Circular RNA_PDHX promotes the proliferation and invasion of prostate cancer by sponging MiR-378a-3p. *Front Cell Dev Biol* **8**: 602707. https://doi.org/10.3389/fcell.2020.602707

Moch H, Srigley J, Delahunt B, Montironi R, Egevad L, Tan PH (2014) Biomarkers in renal cancer. *Virchows Arch* **464**: 359–365. https://doi.org/10.1007/s00428-014-1546-1

Niu M, Shan M, Liu Y, Song Y, Han JG, Sun S, Liang XS, Zhang GQ (2021) DCTPP1, an oncogene regulated by miR-378a-3p, promotes proliferation of breast cancer *via* DNA repair signaling pathway. *Front Oncol* **11**: 641931. https://doi.org/10.3389/fonc.2021.641931

Pan X, Zhao L, Quan J, Liu K, Lai Y, Li Z, Zhang Z, Xu J, Xu W, Guan X, Li H, Yang S, Gui Y, Chen Y, Lai Y (2019) MiR-378a-5p acts as a tumor suppressor in renal cell carcinoma and is associated with the good prognosis of patients. *Am J Transl Res* **11**: 2207–2218

Pan Z, Fang Q, Li L, Zhang Y, Xu T, Liu Y, Zheng X, Tan Z, Huang P, Ge M (2021) HN1 promotes tumor growth and metastasis of anaplastic thyroid carcinoma by interacting with STMN1. *Cancer Lett* **501**: 31–42. https://doi.org/10.1016/j.canlet.2020.12.026

Piva F, Giulietti M, Santoni M, Occhipinti G, Scarpelli M, Lopez-Beltran A, Cheng L, Principato G, Montironi R (2016) Epithelial to mesenchymal transition in renal cell carcinoma: implications for cancer therapy. *Mol Diagn Ther* **20**: 111–117. https://doi.org/10.1007/s40291-016-0192-5

Qin C, Lu R, Yuan M, Zhao R, Zhou H, Fan X, Yin B, Yu H, Bian T (2021) Circular RNA 0006349 augments glycolysis and malignance of non-small cell lung cancer cells through the microRNA-98/MKP1 axis. *Front Cell Dev Biol* **9**: 690307. https://doi.org/10.3389/fcell.2021.690307

Scelo G, Larose TL (2018) Epidemiology and risk factors for kidney cancer. *J Clin Oncol* **36**: Jco2018791905. https://doi.org/10.1200/jco.2018.79.1905

Tang W, Lai YH, Han XD, Wong PM, Peters LL, Chui DH (1997) Murine Hn1 on chromosome 11 is expressed in hemopoietic and brain tissues. *Mamm Genome* **8**: 695–696. https://doi.org/10.1007/s003359900540

Vaupel P, Multhoff G (2021) Revisiting the Warburg effect: historical dogma *versus* current understanding. *J Physiol* **599**: 1745–1757. https://doi.org/10.1113/jp278810

Wang Y, Liu X, Wang L, Zhang Z, Li Z, Li M (2021) Circ_PGPEP1 serves as a sponge of miR-1297 to promote gastric cancer progression *via* regulating E2F3. *Dig Dis Sci* **66**: 4302–4313. https://doi.org/10.1007/s10620-020-06783-5

Wang Y, Zhang Y, Wang P, Fu X, Lin W (2020) Circular RNAs in renal cell carcinoma: implications for tumorigenesis, diagnosis, and therapy. *Mol Cancer* **19**: 149. https://doi.org/10.1186/s12943-020-01266-7

Wang Z, Deng M, Chen L, Wang W, Liu G, Liu D, Han Z, Zhou Y (2020) Circular RNA Circ-03955 promotes epithelial-mesenchymal transition in osteosarcoma by regulating miR-3662/metadherin pathway. *Front Oncol* **10**: 545460. https://doi.org/10.3389/fonc.2020.545460

Yu R, Yao J, Ren Y (2020) A novel circRNA, circNUP98, a potential biomarker, acted as an oncogene *via* the miR-567/PRDX3 axis in renal cell carcinoma. *J Cell Mol Med* **24**: 10177–10188. https://doi.org/10.1111/jcmm.15629

Zhang G, Wang J, Tan W, Han X, Han B, Wang H, Xia Y, Sun Y, Li H (2021) Circular RNA EGLN3 silencing represses renal cell carcinoma progression through the miR-1224-3p/HMGXB3 axis. *Acta Histochem* **123**: 151752. https://doi.org/10.1016/j.acthis.2021.151752

Zhang XO, Wang HB, Zhang Y, Lu X, Chen LL, Yang L (2014) Complementary sequence-mediated exon circularization. *Cell* **159**: 134–147. https://doi.org/10.1016/j.cell.2014.09.001

Zhou Y, Li C, Wang Z, Tan S, Liu Y, Zhang H, Li X (2022) CircRNAs as novel biomarkers and therapeutic targets in renal cell carcinoma. *Front Mol Biosci* **9**: 833079. https://doi.org/10.3389/fmolb.2022.833079

Zhu J, Xiang XL, Cai P, Jiang YL, Zhu ZW, Hu FL, Wang J (2021) CircRNA-ACAP2 contributes to the invasion, migration, and anti-apoptosis of neuroblastoma cells through targeting the miRNA-143-3p-hexokinase 2 axis. *Transl Pediatr* **10**: 3237–3247. https://doi.org/10.21037/tp-21-527